Energy Conversion and Management 266 (2022) 115785

Contents lists available at ScienceDirect

Energy Conversion and Management

journal homepage: www.elsevier.com/locate/enconman

Techno-economic assessment of long-term methanol production from natural gas and renewables

Carlos Arnaiz del Pozo [a], Schalk Cloete [b,*], Ángel Jiménez Álvaro [a]

[a] Universidad Politécnica de Madrid, Spain
[b] SINTEF Industri, Norway

ARTICLE INFO

Keywords:
Methanol
Techno-economic assessment
Energy carrier
Direct air capture
Gas switching reforming

ABSTRACT

Growing climate change concerns are driving interest in alternative energy carriers to fossil fuels. Methanol (MeOH) is a promising candidate to alleviate the challenges faced by hydrogen regarding transportation and storage, with a developed pre-existing infrastructure and a well-known and scalable synthesis process. This study presents a techno-economic assessment of the different avenues for producing MeOH from 1) natural gas and 2) renewable energy with direct air capture (DAC), for effective CO_2 removal from the atmosphere. Under European natural gas prices (6.5 €/GJ), state-of-the-art MeOH production from natural gas reach levelized costs as low as 268.5 €/ton, while an advanced plant using gas switching reforming attains a cost of 252.2 €/ton and approximately 60% lower CO_2 emissions. Middle Eastern costs can drop as low as 135.2 €/ton thanks to low natural gas costs (2 €/GJ). In comparison, renewable MeOH with DAC reach 471.6–784.9 €/ton using technology assumptions representative of the year 2050, with Saudi Arabia achieving the lowest cost thanks to its outstanding solar resource. Overall, renewable MeOH with DAC required CO_2 prices of 121.4–146.7 €/ton to break even with renewable plants using pipeline CO_2, while CO_2 prices in the range of 300 €/ton are required for competitiveness against natural gas routes. Furthermore, a consistent comparison to NH_3 as a carbon-free energy carrier showed that blue and green NH_3 require CO_2 taxes of 49.8 and 274.3 €/ton to break even with natural gas-based MeOH, respectively. However, NH_3 is 14% cheaper than MeOH for renewable pathways, as it avoids the need for DAC. Thus, strong policy support will be required to deploy green MeOH at scale, even in the long-term future.

1. Introduction

Methanol (MeOH) is an industrial commodity used as a building block to produce synthetic hydrocarbons; it is employed as a solvent, energy carrier or directly used as a fuel for transportation [1]. Lately, due to the pressing environmental concerns related to greenhouse gas (GHG) emissions causing global warming [2], focus has been directed towards chemical energy storage systems [3] to facilitate decarbonization efforts. Different chemical compounds have been considered for this purpose, with hydrogen receiving an increasing interest as it constitutes a carbon-free energy carrier [4]. However, storage and transportation of this molecule presents substantial challenges in terms of large-scale feasibility [56], with no existing infrastructure available. MeOH, on the other hand, can be transported at ease in liquid state at ambient temperatures through a well-developed pre-existing value chain, and presents low toxicity and safety hazards, showing substantial potential to increase its presence in a future decarbonized economy as an intermediate energy storage medium [7]. MeOH and its derivatives are attractive fuels for the transport sector [8], while it also has the potential to be utilized as gas turbine fuel [9] in peak electricity production, or as a hydrogen carrier for fuel cell technology [10].

The MeOH economy offers the advantage that all energy sources, of fossil and renewable origin, can be employed to produce this compound. The source of the carbon atom can be a recovered CO_2 molecule originating from emissions of industrial and power plant sites through carbon capture utilization (CCU), while H_2 can be effectively supplied by means of electrolysis of water with renewable power supply. This production pathway can potentially enable effective mitigation of CO_2 emissions at large capacities; Rivera-Tinoco et al. [11] predict MeOH costs of 891 €/ton and 5459 €/ton using proton exchange membrane (PEM) and solid oxide (SOEC) water electrolysis, respectively. However, Ravikumar et al. [12] highlights that it is environmentally preferable to supply renewable electricity to the grid rather than MeOH production from CCU, unless the grid CO_2 intensity drops below 67 $kgCO_2$/MWh. Kotowicz et al. [13] report an energy efficiency between 45.5% and 52.9%

* Corresponding author.
E-mail address: schalk.cloete@sintef.no (S. Cloete).

https://doi.org/10.1016/j.enconman.2022.115785
Received 2 April 2022; Received in revised form 13 May 2022; Accepted 17 May 2022
Available online 26 May 2022

Nomenclature

Acronyms

ATR	Autothermal reformer
ARG	Argentina
ASME	American Society of Mechanical Engineers
ASU	Air Separation Unit
BEC	Bare erected cost
BWR	Boiling water reactor
CCU	Carbon capture & utilization
CLR	Chemical looping reforming
CPU	Cryogenic purification unit
DAC	Direct air capture
EPC	Engineering, procurement and construction
ESP	Spain
FTR	Fired tubular reformer
FOM	Fixed operating & maintenance costs
GAMS	General algebraic modelling system
GER	Germany
GHG	Greenhouse gas
GSR	Gas switching reforming
HTER	Heat transfer exchanger reformer
IPCC	Intergovernmental panel on climate change
IP	Intermediate pressure
LP	Low pressure
LCOM	Levelized cost of methanol
LCOP	Levelized cost of product
LHV	Lower heating value
LNG	Liquefied natural gas
LP	Low pressure
OC	Owners costs/Oxygen carrier
PEM	Proton exchange membrane
PC	Process contingency
PT	Project contingency
P/L	Pipeline
CCU	Carbon capture utilization
SEA	Standardized economic assessment
SMR	Steam methane reformer
SOEC	Solid Oxide Electrolyte Cell
TOC	Total overnight cost
tpd	Tons per day
VOM	Variable operating & maintenance cost
WGS	Water gas shift

List of symbols

M	Syngas module
η	Thermal efficiency
ε	Molar efficiency
k	Kinetic constant
K_{eq}	Equilibrium constant
E_{CO_2}	Specific emissions
SC	Specific consumption (GJ/ton)
$\dot{m}$	Mass flow (kg/s)
$\dot{n}$	Molar flow (mol/s)
P	Pressure (bar)
$\dot{W}$	Power (kW)

for MeOH production from a wind farm and CO_2 from power plants, while Battaglia et al. [14] calculates costs of 846 €/ton of MeOH for hydropower energy source and CO_2 from a coal thermal plant for small scale production capacities of around 20 tpd. Alternatively, CO_2 can be captured directly from air (DAC). This avenue was investigated by Bos et al. [15] for a standalone 100 MW wind power MeOH process, achieving costs of 750–800 €/ton. Much more optimistic outlooks are also available such as Schorn et al. [16] predicting renewable MeOH costs of 370-600 €/ton for H_2 prices ranging from 1.35 to 2 €/kg and CO_2 production (from DAC) at a cost of 100 €/ton, for the year 2030.

On the other hand, MeOH production through conversion of natural gas can present an alternative means of energy storage for transportation relative to liquefaction, in which case fuel efficiency, capital investment and CO_2 emissions reduction of the production process become increasingly important. In this respect, several avenues for the enhancement of the process are envisaged. New reactor technologies beyond gas phase reactors based on Cu catalysts have the potential to increase conversion per pass of reactants achieving energy savings and cost reductions of the synthesis loop [17]. Liquid phase reactors can allow a more efficient removal of the heat of reaction [18], but are limited by greater catalyst deactivation rates [19]. Alternatively, membrane reactor technologies enable the withdrawal of products from the reaction to improve the yield and reduce investment costs [20,21].

Cost reduction and efficiency enhancement opportunities can also be attained in the syngas generation section. One such possibility is chemical looping reforming (CLR) [22], which can provide a suitable syngas stream to the synthesis process. An alternative operation using dynamically operated fluidized beds with a valve switching mechanism [23] avoids the challenges of pressurized operation of interconnected fluidized beds and effectively decouples the oxidation, reduction and reforming steps undergone by the metallic oxygen carrier. Nazir et al. [24] propose a gas switching reforming (GSR) concept for high efficiency H_2 production from natural gas with inherent CO_2 capture, leading to H_2 costs as low as 1.83 $/kg. Experimental demonstration of GSR was conducted by Wassie et al. [25].

Osman et al. [27] presents an experimental and process simulation study using CLR for MeOH production, revealing equivalent efficiency improvements of 5.3% relative to conventional production through autothermal reforming. In terms of economics, Spallina et al. [28] presents a detailed techno-economic study of the dynamically operated packed bed CLR reactors integrated with a MeOH synthesis conversion loop, achieving cost reductions relative to conventional synthesis pathways of 64.9 $/ton, while Labbak et al. [29] presents levelized costs as low as 242 $/ton for a CLR based MeOH production process configuration with Pressure Swing Adsorption (PSA). Other novel alternatives of the syngas generation section for MeOH production include tri and dry reforming of methane enabling a large reduction of CO_2 emissions from the plant through an enhanced CO_2 conversion, relative to SMR configurations for syngas production and downstream CO_2 addition [30].

Due to the different economic and modelling assumptions between literature sources, it is compelling to carry out a detailed techno-economic study of the different MeOH production pathways from a consistent baseline. Such is the purpose of the present work, where the alternative avenues of MeOH production from natural gas using conventional technologies are presented in detail and discussed, as well as a potential advanced process based on CLR, and subsequently benchmarked against renewable production by water electrolysis from renewable energy and DAC. Several studies considering different locations, technology costs and alternative CO_2 sources (utilization of captured CO_2 from thermal power or industrial plants) for the renewable case are also presented to provide a holistic perspective of the potential of each synthesis route.

1.1. Technology overview

A brief description of the MeOH processes considered in this work is depicted here, to highlight the core technological features of each

concept. A block flow diagram of the different plant configurations is shown in Fig. 1.

- Fig. 1 A) represents an SMR-ATR plant, where the syngas is produced through steam methane reforming followed by autothermal reforming. This plant was studied by Blumberg et al. [31], Spallina et al. [28] and Collodi et al. [32] and it has been deployed for capacities up to 5000 tpd. The key feature is that the purge stream from the synthesis loop is employed as fuel to provide heat for the reforming, while the steam generation is carried out from heat recovery of the ATR effluent.
- Fig. 1 B) outlines the ATR-HTER plant where syngas is produced from autothermal reforming and a heat transfer exchanger reformer [33] is employed to effectively recover heat from the ATR outlet for conversion of a portion of the natural gas. This syngas production pathway is the preferred choice in modern MeOH plants for large capacities [34]. Assessments employing a single ATR for MeOH production are presented by Woods et al. [35] and Blumberg et al. [36]. The integration of the HTER enables an improved thermal performance, lower O_2 consumption and convenient operating handle to adjust the syngas module for MeOH synthesis.
- Fig. 1 C) shows the GSR concept based on chemical looping technology. It effectively integrates the synthesis loop purge stream with the reduction step of the cluster while retrieving most of the CO_2 contained in the reduction outlet and recycling it to the reformer for minimal carbon loss. Techno-economic assessments using the same syngas production principles were carried out by Labbak et al. [29], Spallina et al. [28] and Osman et al. [27].
- Fig. 1 D) depicts the renewable MeOH concept utilizing electrolyser technology and direct air capture (DAC) or, alternatively, CO_2 from fossil fuel origin available from pipeline. Given the two alternative CO_2 sources, the corresponding scope is shown in discontinuous lines for this configuration. Concepts using DAC for MeOH synthesis have been previously studied by Bos et al. [15], revealing poor competitive prospects relative to fossil fuel routes.

In the following sections, a comprehensive description of the three natural gas MeOH routes and the renewable MeOH production pathway is presented, providing details of the synthesis loop topology and reactor model employed, common to all models. Then, the key performance indicators from an energy and environmental perspective are defined while the economic methodology is outlined. Subsequently, the techno-economic results for all plants are shown, with appropriate sensitivity analysis to relevant economic assumptions and benchmarking between the different production pathways. Finally, the main outcomes of the study are summarized and the core conclusions are drawn.

2. Methodology

In this section, each of the plant characteristics are discussed in detail. Stationary power plant models were built in Unisim Design R481 for the natural gas-based plants and some components of the renewable MeOH case. The Peng-Robinson equation of state (EoS) was used for thermodynamic property estimation in the syngas generation section as recommended by the user manual for natural gas and air components [37]. ASME steam tables were used in the steam power cycle components and Soave Redlich-Kwong EoS in the synthesis loop [36]. The GSR dynamic model is built in Scilab with property estimation from an in-house thermodynamic database from Universidad Politécnica de Madrid (Patitug) and integrated in the stationary flowsheet through a CAPE-OPEN unit operation. The natural gas-based plants are assessed using process modelling followed by an economic assessment. The renewable plants require optimization of the investment and hourly dispatch of each candidate technology to produce a constant MeOH output at minimal costs from the intermittent supply of power. The methodology of the assessment for the different cases is depicted in Fig. 2:

2.1. Natural gas MeOH plants

This section provides a technical description of the MeOH plant from natural gas. The key differences reside in the syngas generation route and process design features to attain a suitable module for the synthesis loop. All plants are designed adjusting the natural gas intake in each case to produce approximately 10,000 tpd of MeOH, which corresponds to the largest projected production capacity achievable [34]. Detailed process diagrams and stream summaries can be found in the Supplementary Material file attached to this work.

2.1.1. SMR-ATR

In the SMR-ATR plant, a fired tubular reformer (FTR) operating with a steam to carbon ratio of 1.8 [34] at 25 bar partially converts methane to carbon monoxide and hydrogen, after a pre-reforming and desulphurization steps. Since the steam methane reaction produces a H_2/CO ratio of 3, the reaction is limited by a low operating temperature in the reformer tube outlet. The syngas effluent is then routed to an autothermal reformer (ATR) where it is partially combusted with 95%mol pure O_2 from an air separation unit (ASU), providing heat for further reforming in the catalyst section of the ATR. The outlet temperature of the ATR is controlled with the oxygen intake flow to maintain a low methane slip, which is detrimental for the synthesis loop performance as it accumulates in the recycle stream and thus reduces the conversion per pass. On the other hand, the temperature outlet from the FTR fixes the module of the syngas product to the synthesis requirements (see Eq. (3)). After the ATR, a heat exchanger network delivers HP superheated steam, IP reheated steam, IP water and LP steam to the steam turbine, MeOH loop and purification column reboiler. After water knock out, syngas is compressed to 100 bar and routed to the synthesis loop. The purge fraction from the loop recycle stream (around 4.5%) is selected to supply sufficient heat to the FTR reformer upon combustion with close to stoichiometric air, fed to the system with a blower. The hot gas from the furnace at 1010 °C is used to preheat the incoming natural gas stream in a series of heat exchangers. Since the synthesis loop contains unconverted CO and CO_2, as well as CH_4 from the reformer, the combustion of this stream implies generation of CO_2 emissions and therefore a reduction of the carbon conversion to MeOH.

2.1.2. ATR-HTER

In the ATR-HTER plant configuration, syngas at 25 bar is produced employing an autothermal reformer (ATR) fed with O_2 from an ASU. The high temperature and low S/C (0.6) operation achieves a low methane slip and low CO_2 formation. The outlet stream is routed to a heat transfer exchanger reformer (HTER) [38] operating in parallel disposition with the ATR. Namely, 20% of the natural gas input is reformed at a higher S/C (2.7) in reformer tubes with heat provided by the ATR outlet and the reformed product of the HTER. Such an arrangement facilitates a suitable module close to 2. The mixed effluent is then cooled down by preheating the inlet natural gas streams to the HTER and ATR in a recuperator. The syngas product is further cooled in a series of heat recovery exchangers to produce steam and hot water. After a final heat rejection to ambient temperature, condensed water is knocked out and the syngas is compressed to 75 bar and routed to the synthesis loop. A somewhat lower pressure operation is selected for the synthesis loop for a fixed reactor volume because the large ratio of CO/CO_2 in the syngas, relative to the other models, provides a quality syngas with high reactivity, resulting in comparatively higher conversions per pass. Furthermore, since the reverse water gas shift reaction (WGS) takes place to a small extent due to the lower presence of CO_2 in the feed, there is a lower concentration of water in the raw MeOH product, reducing the size and energy demand of the purification column. The purge fraction from the synthesis loop recycle stream (4.4%) is specified to achieve sufficient power generation in a steam boiler power cycle to satisfy the plant

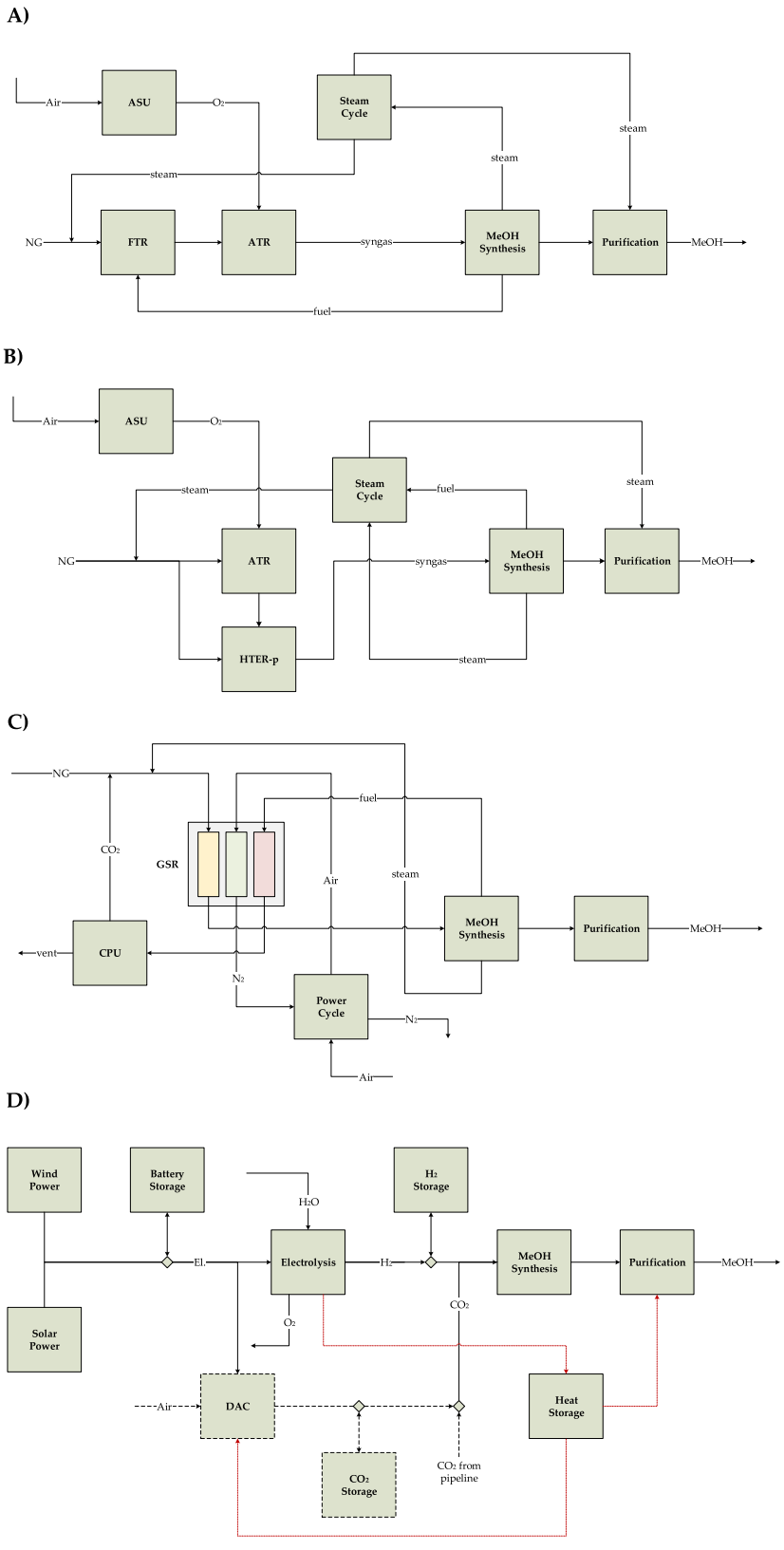

Fig. 1. Block flow diagram of the different MeOH production pathways: SMR-ATR (A), ATR-HTER (B), GSR (C), and renewable (D). Yellow, green, and red columns in the GSR cluster represent reforming, oxidation, and reduction steps respectively. In the renewable plant, red lines represent heat flows and dashed black lines alternative CO_2 supply pathways. (For interpretation of the references to colour in this figure legend, the reader is referred to the web version of this article.)

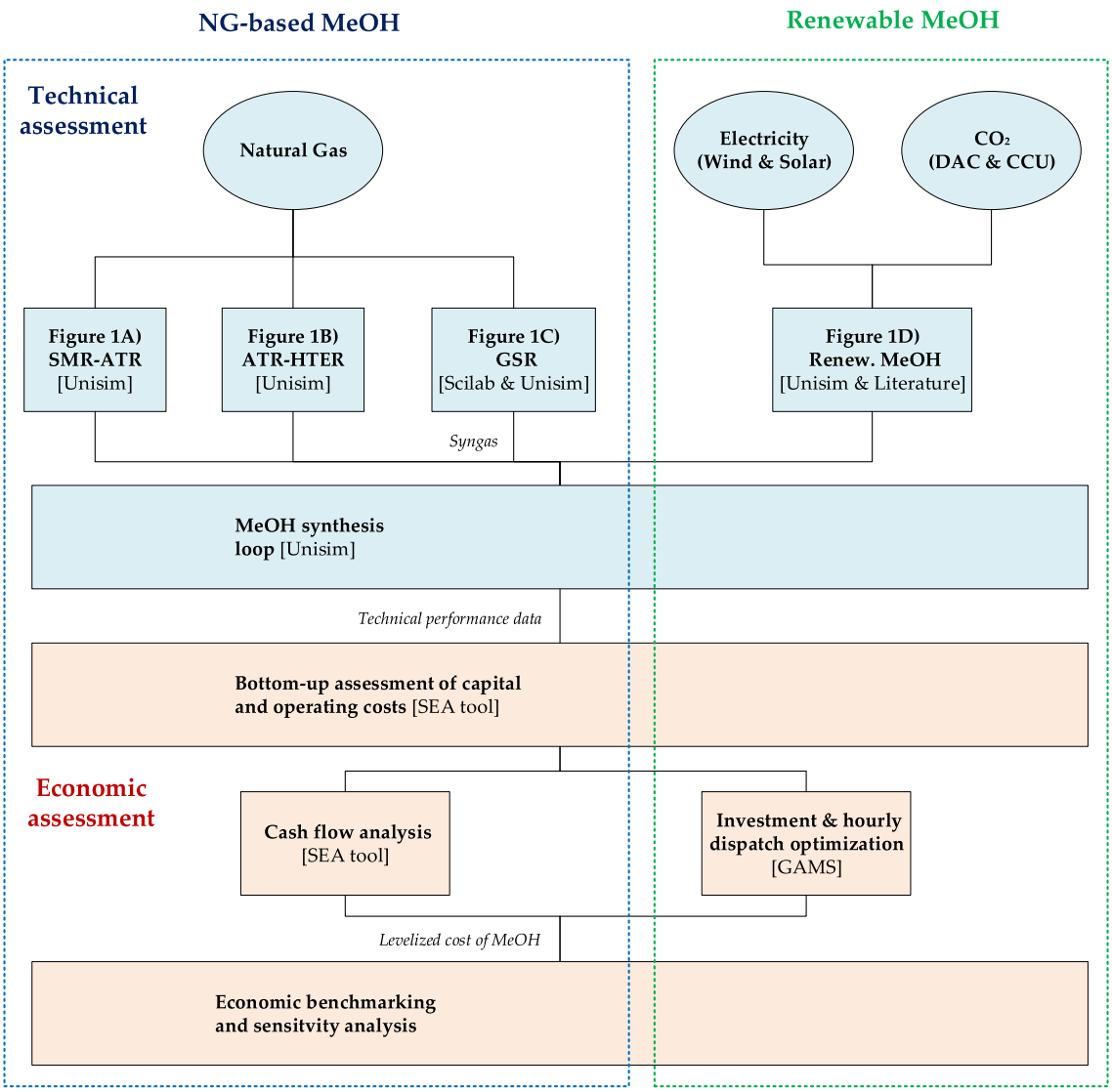

Fig. 2. Methodology framework of this study.

auxiliary demand. This implies emissions arising from the combustion of carbonaceous species present in the fuel. A steam extraction from the LP stage delivers sufficient steam to the purification reboiler column to meet the demand.

2.1.3. GSR

This work explores a MeOH production configuration based on such a syngas generation concept using a Ni-based oxygen carrier [26] and reactor operating temperatures reaching a maximum value of 1030 °C, a conservative value which strengthens the feasibility prospects of high temperature gas switching valves and filters. The GSR plant features a dynamically operated fluidized bed cluster of reactors to generate syngas for the synthesis reaction. Similarly to previous work [39], steel rods are placed within the reactor volume to provide thermal mass, minimizing temperature fluctuations across the cycle, which increases the average reforming temperature leading to higher methane conversion. The topology proposed here presents similarities to the concepts studied by Spallina et al. [28], but incorporates several modifications. First, the maximum GSR cycle operating temperature is adjusted to close the energy balance with the purge stream heating value (employed in the GSR reduction step, Fig. 1C). All the steam produced by the MeOH reactor is supplied to the GSR reforming inlet, practically avoiding a steam turbine and condenser. The resulting maximum temperature required in the present model was 1030 °C, in line with previous conservative assumptions for this technology from the authors [39], and similar to the values reported by Spallina et al. [28]. The purge fraction (5.1%) is specified to attain a reasonable recycle to feed ratio in the synthesis loop, similarly to the conventional plants. At a temperature of 1030 °C, these specifications are met while achieving sufficiently high methane conversion (88.6%) to avoid a large accumulation of this component in the synthesis loop. Secondly, the GSR cluster is operated to minimize ingress of N_2 to the reforming step outlet, avoiding undesirable presence of this inert species in the syngas product. Finally, the reduction outlet, containing a relatively large concentration of N_2 after water knock out (around 30%) due to mixing in the GSR, is routed to a cryogenic purification unit [40], where approximately 80% of the CO_2 is retrieved at a purity of 97%mol. This stream is repressurized to GSR pressure and reheated before being mixed with the preheated natural gas and stream inlet to the reformer, allowing to adjust the module conveniently for the synthesis reaction. By carrying out the purification prior to the recycling to the reformer inlet, further reductions of the N_2 concentration in the syngas are attained. The reforming outlet is cooled down by preheating the incoming streams, while LP steam and IP water for the MeOH reactor is produced in a downstream multi-stream heat exchanger. The

oxidation outlet, after expansion in a turbine, is routed to a heat exchanger further producing LP steam. The higher content of CO_2 in the syngas requires a larger separation column than in conventional plants due to the increased production of water in the synthesis.

2.2. Renewable MeOH plant

The renewable MeOH plant considered in this work utilizes power from intermittent wind and solar power resources to split water molecules to oxygen and hydrogen in an electrolyser (PEM), operating with an LHV efficiency of 70%, extrapolated from European targets [41], and an H_2 production pressure of 30 bar. Research and development efforts towards higher temperature operation (150 °C) [11] at pressurized conditions can improve system efficiency by reducing overvoltage losses [42]. The assumption that such elevated temperature electrolysis becomes commercially viable in the future is important for satisfying the process heat demand, as outlined later. On the other hand, two alternatives are considered for recovering the CO_2 for the synthesis reaction. First, a direct air capture system based on low temperature solid amine sorbents (Fasihi et al. [43]) to produce true green MeOH. CO_2 from DAC is assumed to be produced at a vacuum pressure of 0.2 bar and a 99.9% mol purity [44]. Further compression to synthesis pressure is performed by means of a three-stage intercooled compressor. Due to the lack of constant wind and solar power availability, storage devices of electricity, hydrogen, CO_2, heat and MeOH must be deployed to maintain a steady output of MeOH from the plant fixed to a value of 2300 MW. Heat from this elevated temperature electrolysis process is effectively employed to match the large thermal demand of the DAC regeneration step and the MeOH purification section, by means of intermittent steam storage [45], under the assumption that electrolyser waste heat can be used to generate low pressure steam at 150 °C. Furthermore, the model also incorporates the possibility of using excess renewable energy capacity to generate more steam through resistance heating, allowing for a more optimal energy integration of the scheme. Alternatively, electricity can be stored in batteries, while CO_2 and H_2 must be compressed and stored in pressurized tanks.

The second configuration produces MeOH without the technological uncertainties of DAC and elevated-temperature electrolysis. In this configuration, pressurized CO_2 originating from CO_2 capture from large point sources is delivered via pipeline (CCU) and assigned a CO_2 utilization credit for avoiding additional pipeline and CO_2 storage infrastructure. In exchange for the large process simplification and technology risk reduction of this plant, the MeOH product can no longer be considered green as the CO_2 would originate mainly from fossil sources. However, the produced liquid fuel can still displace liquid fuel from fossil origins.

The synthesis loop for the renewable cases is operated at 100 bar, due to the lower reactivity of the syngas relative to that produced from natural gas autothermal reforming, producing large amounts of water because of the high reaction extent of the reverse WGS. This requires a larger distillation column to meet the purity requirements, relative to the other plants. A small backpressure steam turbine utilizing the synthesis heat of reaction for steam evaporation is used to produce some electricity, while hot water to the BWR is supplied by heat recovery from the compressor intercoolers. The low-pressure steam output at 1.8 bar is used to partially satisfy the column reboiler duty. In the case with CO_2 supply via pipeline, the synthesis loop is simplified by avoiding the need for CO_2 compressors and buffer storage.

2.3. Synthesis loop

The synthesis loop employed for MeOH production is depicted in Fig. 3. The system consists of an isothermal boiling water reactor [17], where the exothermic heat of reaction is transferred across the tube length to produce steam at 32 bar and 250 °C. An homogeneous reactor model of a catalyst packed bed is employed to calculate the conversion

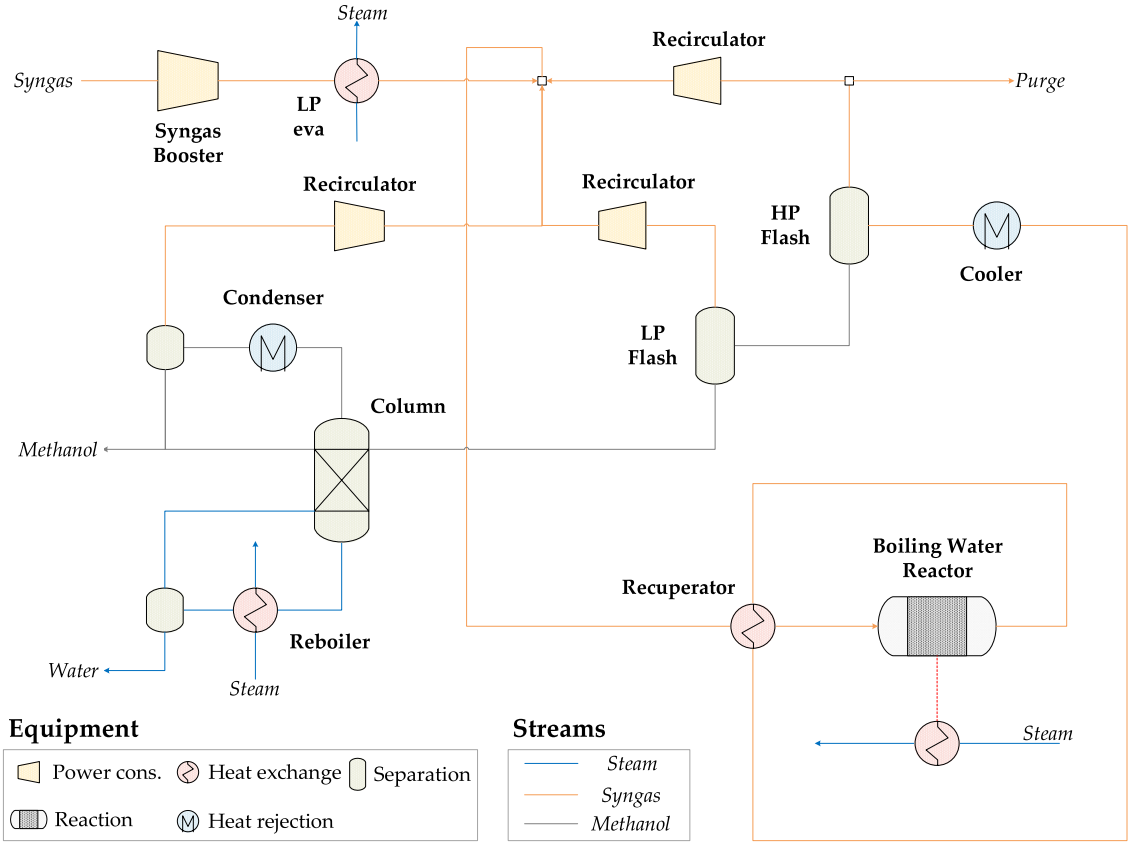

Fig. 3. MeOH synthesis and purification loop.

of reactants, achieving very close predictions to more involved heterogenous models taking into account mass and energy balances in the solid phase, as shown by De María et al. [46]. This study considers that the MeOH synthesis follows the reaction mechanism of CO_2 hydrogenation and (reverse) water gas shift (WGS) reaction, as illustrated in Eq. (1) and Eq. (2).

$$CO_2 + 3H_2 \leftrightarrow CH_3OH + H_2O \tag{1}$$

$$CO + H_2O \leftrightarrow H_2 + CO_2 \tag{2}$$

For optimal operation of the synthesis loop, it is required that the reactants are fed at close to the stoichiometric ratio or module M of 2, defined by Eq. (3).

$$M = \frac{[H_2] - [CO_2]}{[CO] + [CO_2]} \approx 2 \tag{3}$$

Several kinetic models are available for industrial MeOH synthesis [47]). The kinetic expressions specified in the reactor model in this study were derived by [48] over a Cu/ZnO/Al_2O_3 catalyst, and are reflected in Eq. (4) and Eq. (5). These expressions are selected for their relative simplicity, with the pre-exponential constants and activation energies for the kinetic constants $k_{j,i}$ and the equilibrium constant expressions $K_{eq,j}$ detailed in the aforementioned study [48]. However, kinetics assuming different active sites for both CO and CO_2 hydrogenation are also suitable for applications with varying ratios of these molecules [49]). Nevertheless, the chosen kinetic model will more accurately reflect the impact of differences in syngas composition across the plants compared to an equilibrium conversion approach as used in several large-scale technoeconomic studies (e.g.,[27,28]). Furthermore, the use of a kinetic model ensures that full equilibrium conversion is not achieved and that the reactor can be accurately sized for the capital cost estimation. Further assumptions of the reactor model are provided in Table 1.

$$r_{MeOH} = \frac{k_{1,1} P_{CO_2} P_{H_2} \left[1 - \frac{1}{K_{eq,1}} \left(\frac{P_{H_2O} P_{CH_3OH}}{P_{CO_2} P_{H_2}^3}\right)\right]}{\left(1 + k_{1,2}\frac{P_{H_2O}}{P_{H_2}} + k_{1,3} P_{H_2}^{0.5} + k_{1,4} P_{H_2O}\right)^3} \tag{4}$$

$$r_{rWGS} = \frac{k_{2,1} P_{CO_2} \left[1 - K_{eq,2} \left(\frac{P_{H_2O} P_{CO}}{P_{CO_2} P_{H_2}}\right)\right]}{\left(1 + k_{2,2}\frac{P_{H_2O}}{P_{H_2}} + k_{2,3} P_{H_2}^{0.5} + k_{2,4} P_{H_2O}\right)} \tag{5}$$

The reactor is operated under typical industrial process conditions [17]: the inlet feed to the reactor is set to 230 °C, allowing for an adiabatic section where the heat of reaction elevates the temperature to 260 °C, after which the heat transfer fluid (boiling steam) removes heat to maintain constant temperature on the reaction side thereby maximizing conversion per pass. Such a narrow temperature range is maintained to ensure a long catalyst lifetime and stable operation avoiding deactivation [50]. The loop is designed at high pressure (75–100 bar) to minimize recirculation of material due to incomplete conversion of the reactants, ensuring a reactor inlet to fresh feed gas molar ratio of ~3.5–3.8, thereby attaining a low pressure drop per pass to reach low recompression power. Formal optimization of the synthesis loop pressure was not attempted, but the effect would likely be small due to several counterbalancing effects. For example, lowering the synthesis loop pressure will decrease syngas compression costs but also reduce conversion per pass, increasing efficiency losses related to a larger recycle and purge.

Table 1
Reactor modelling details.

Item	Value	Units
Inlet temperature	230	°C
Outlet temperature	260	°C
Pressure drop	Ergun	–
Catalyst density	1770	kg/m3
Catalyst particle diameter	0.005	m
Void fraction	0.4	–
Tube length (adiabatic section)	1.5–2	m
Tube length (isothermal section)	9	m
Tube diameter	0.085	m

As illustrated in Fig. 3, the fresh syngas from the reforming section of each plant is compressed to high pressure in an adiabatic stage and mixed with the recirculating streams. The mixture is heated up in the recuperator prior to entering the boiling water reactor employed for MeOH production, the effluent of which exchanges heat with the inlet. This outlet stream is further cooled to ambient temperature and then routed to a high pressure knock out vessel where condensed MeOH product and water are withdrawn, together with a gaseous stream which is recycled to the feed point via a recompression stage to overcome the pressure losses of the loop. The liquid product is expanded to 2 bar and sent to a low-pressure vessel, after which the flashed vapours are recompressed and mixed with the feed. The liquid effluent is sent to a purification column (with changing n° of trays for each plant) where the raw MeOH is purified to 98%mol for bulk transportation achieving almost complete recovery. LP steam at 1.8 bar from different plant sections (steam turbine extraction, dedicated boilers) supplies sufficient heat to the reboiler, achieving approximate heat demand of 2.4–2.6 MJ/kg of MeOH, in line with Halager et al. [51], depending on the amount of water in the feed to the distillation section. The column presents a partial condenser producing MeOH at 60 °C, while the off gas is again recirculated to the feed point of the synthesis loop after recompression.

2.4. Plant performance indicators

Energy, environmental and economic performance indicators are defined in this section to facilitate a holistic comparison between the different MeOH production pathways.

2.4.1. Energy and environmental

Thermal efficiency is defined as the MeOH product lower heating value and the natural gas lower heating value input as shown in Eq. (6). The equivalent efficiency Eq. (7) accounts for electricity consumption or exports of the plant assuming a benchmark natural gas combined cycle efficiency of 62.3% [52], considering that work imported to the plant has a negative sign. The electrical efficiency is defined with the net power production of the plant in Eq. (8).

$$\eta_{MeOH} = \frac{\dot{m}_{MeOH} LHV_{MeOH}}{\dot{m}_{NG} LHV_{NG}} \tag{6}$$

$$\eta_{MeOH,eq} = \frac{\dot{m}_{MeOH} LHV_{MeOH}}{\dot{m}_{NG} LHV_{NG} - \frac{\dot{W}_{net}}{\eta_{CC}}} \tag{7}$$

$$\eta_{El.} = \frac{\dot{W}_{net}}{\dot{m}_{NG} LHV_{NG}} \tag{8}$$

On the other hand, carbon and hydrogen efficiencies as shown in Eq. (9) and Eq. (10), respectively, indicate the fraction of the respective atoms from the original fuel that are present in the final product. It gives an understanding of the conversion efficiency of the different process designs:

$$\varepsilon_C = \frac{\dot{n}_{C,MeOH}}{\dot{n}_{C,NG}} \tag{9}$$

$$\varepsilon_H = \frac{\dot{n}_{H,MeOH}}{\dot{n}_{H,NG}} \tag{10}$$

Complementary metrics in terms of specific consumption Eq. (11) and specific equivalent consumption Eq. (12) are provided to reflect the energy investment required per mass unit of product, without and with electrical input/output in the calculation, respectively.

$$SC = \frac{\dot{m}_{NG} LHV_{NG}}{\dot{m}_{MeOH}} \tag{11}$$

$$SC_{eq} = \frac{\dot{m}_{NG,eq} LHV_{NG} - \frac{\dot{W}_{net}}{\eta_{CC}}}{\dot{m}_{MeOH}} \tag{12}$$

Environmental metrics refer to the specific CO_2 emissions per unit of product, as reflected in Eq. (13).

$$E_{CO_2} = \frac{\dot{m}_{CO_2,emit.}}{\dot{m}_{MeOH}} \tag{13}$$

For the renewable MeOH plants, similar efficiencies are defined in Eq. (14) to Eq. (17), but taking into account the primary energy input consists of renewable electricity. Here, both the electrolyser consumption and the DAC power demand (if implemented) are considered in the denominator, while the subsequent reactant and recycle loop compression auxiliary consumption is considered in the equivalent metric definition, taking into account this power demand of the conversion process.

$$\eta_{MeOH} = \frac{\dot{m}_{MeOH} LHV_{MeOH}}{\dot{W}_{Elect.} + \dot{W}_{DAC}} \tag{14}$$

$$\eta_{MeOH,eq} = \frac{\dot{m}_{MeOH} LHV_{MeOH}}{\dot{W}_{Elect.} + \dot{W}_{DAC} + \dot{W}_{SL}} \tag{15}$$

$$SC = \frac{\dot{W}_{Elect.} + \dot{W}_{DAC}}{\dot{m}_{MeOH}} \tag{16}$$

$$SC_{eq} = \frac{\dot{W}_{Elect.} + \dot{W}_{DAC} + \dot{W}_{SL}}{\dot{m}_{MeOH}} \tag{17}$$

2.4.2. Economic

The economic assessment of the MeOH plants was conducted with the Standardized Economic Assessment (SEA) tool developed by the authors [53]. The tool performs a capital cost estimation of each process unit in the plant using cost-capacity correlations and Turton equations [54], adjusting the source to the target cost basis outlined in Table 2. A user manual is available for download [55]. Furthermore, the tool incorporates location factors to account for material and labour cost differences in several world regions [56].

The assumptions for total overnight cost (TOC), fixed (FOM) and variable (VOM) operating costs estimation and the cash flow analysis are presented in Table 3. All plant units employ a process contingency factor of 0%, except in the advanced GSR reforming section for which a 20% is assumed.

Several sensitivity analyses of the LCOM to key economic assumptions are carried out for the NG-based MeOH plants including the effect of variations in the price of natural gas, the CO_2 tax imposed on emissions, electricity price, oxygen carrier cost and cash flow analysis assumptions such as discount rate and capacity factor. Each parameter is varied independently, keeping the remaining at their base reference value.

The natural gas MeOH plants are benchmarked against renewable MeOH deployed in several world regions with different solar and wind availability profiles, taken from the Renewables Ninja online tool [58]. Table 4 reveals wind and solar resources in Argentina (ARG), Germany (GER), Spain (ESP) and Saudi Arabia (SA). Different trends are identifiable amongst the locations: availability is more constant in SA throughout the year, while the solar resources in GER vary more strongly between winter and summer, despite complementary wind variation partially offsetting this. On the other hand, ARG (the Patagonian region) enjoys an extraordinarily high wind availability. This latter region was not benchmarked directly with co-located natural gas-based plants under the assumption that fuel prices will be similar to Europe.

Similarly to the NG-based plants, sensitivity studies to key economic assumptions were performed to the renewable MeOH plants for each location, as reflected in Table 5. Wind, solar and electrolyser capital cost variations were considered to vary in the range of -+30%. Furthermore, DAC projected capital costs and thermal/electricity demand from [59] for 2050 were assumed as an optimistic case while the conservative case employs the costs reported in that study for 2020. The base assumption taken in the present work is the average over these values, given that the 2050 cost forecast results in extremely low levelized costs of DAC (50 €/ton), presuming that DAC systems will become profitable technologies operating in isolation, given the CO_2 taxes assumed in this study of 100 €/ton. Additionally, the cost difference between the base configuration

Table 2
Targe cost basis details.

Location	Western Europe
Year	2020
Currency	€

Table 3
Economic evaluation assumptions [35,56,57].

Capital estimation methodology		
Bare Erected Cost (BEC)		SEA Tool Estimate
Engineering Procurement and Construction (EPC)		10% BEC
Process contingency (PC)		0–20% BEC
Project Contingency (PT)		20% (BEC + EPC + PC)
Owners Costs (OC)		15% (BEC + EPC + PT + PC)
Total Overnight Costs (TOC)		BEC + EPC + PC + PT + OC
Operating & maintenance costs		
Fixed		
Maintenance	2.5	%TOC
Insurance	1	%TOC
Labour	60,000	€/y-p
Operators	50–60	Persons
Variable		
Natural gas	6.5	€/GJ
Electricity	60	€/MWh
Oxygen carrier	15	€/kg
Reformer catalyst	15	€/kg
MeOH reactor catalyst	30	€/kg
CO_2 tax	100	€/ton
Process water	6	€/m^3
Cooling water make-up	0.35	€/m^3
Cash flow analysis assumptions		
1st year capacity factor	65	%
Remaining years	85	%
Discount Rate	8	%
Construction period	4	years
Plant Lifetime	25	years

Table 4
Regional economic assumption for renewable MeOH plants.

Item/Location	Argentina (ARG)	Germany (GER)	Spain (ESP)	Saudi Arabia (SA)
Wind capacity factor (%)	54.4	29.5	34.5	32.6
Solar capacity factor (%)	12.7	12.4	19.3	21.8
Natural gas price (€/GJ)	–	6.5	6.5	2
Electricity price (€/MWh)	–	60	60	40

Table 5
Sensitivity analysis ranges for the renewable MeOH plants.

Item/Level	Low	High
Electrolysis, Wind & Solar	−30%	30%
DAC*	[43] (forecast 2050)	[43] (forecast 2020)

*Includes corresponding variations in thermal (±22.7%) and electricity (±15.7%) demand.

and an alternative synthesis pathway with CO_2 utilization from a pipeline at the required hourly rate is also presented, taking into consideration a credit for avoiding CO_2 storage of 10 €/ton. Furthermore, in the suitable locations, the difference with respect to the GSR MeOH plant is also outlined for an overall perspective.

3. Results

The results of this work are presented in two sections. First, the energy breakdown and performance of the plants attending to energy and environmental metrics earlier defined are presented and discussed. Secondly, the economics of the different production routes is discussed, providing sensitivity cases to key assumptions of the analysis.

3.1. Energy and environmental results

Table 6 shows the energy and environmental results for the different MeOH plants. When looking at the two-reference natural gas-based plants, the configuration based on ATR-HTER for syngas production achieves marginally better specific consumption and thermal efficiencies relative to the SMR-ATR process. This results because the latter has a fixed duty requirement imposed by the FTR section of the plant which results in excess electricity production through a low efficiency Rankine cycle, while the former can adjust the purge stream to produce close to the amount required by the plant. This in turn translates to slightly higher fuel consumption and ultimately higher specific emissions for the SMR-ATR case. On the other hand, the GSR MeOH plant achieves a better fuel utilization which translates to approximately 6.2 %-points higher MeOH efficiency and 2.2 GJ/ton lower specific consumption relative to the ATR-HTER case. This attractive thermal performance is somewhat offset by the electricity imports required by the GSR plant; in terms of equivalent efficiency and specific consumption this plant still outperforms the ATR-HTER benchmark by 3.2 %-points and 1.2 GJ/ton respectively. However, due to the effective integration of the CPU purified stream in the reforming inlet to the GSR, carbon conversion efficiency of the scheme is approximately 6 %-points higher than the benchmark plant, which leads in turn to 2.6 times lower specific CO_2 emissions. Due to the good performance of the chemical looping system to integrate the purge heat for natural gas reforming, the resulting hydrogen efficiency is above 100%, due to the steam present in the feed.

Noticeably, the GSR configuration presents both a lower total auxiliary power consumption and power generation relative to both references. This is primarily a consequence of avoiding an energy intensive air separation unit, through the alternative steps oxidation/reduction of the oxygen carrier which indirectly supply heat for reforming. Furthermore, the GSR concept also practically avoids a bulky steam cycle relative to the reference plants, producing most of its electrical power through the gas turbine coupled to the GSR. Finally, the Renewable MeOH plant shown in Table 6 incorporates DAC power demand to achieve a pure CO_2 stream for synthesis. The results reveal a relatively low electricity to MeOH efficiency, a high carbon conversion (only a small amount of CO_2 is vented through a small purge stream to prevent small amounts of N_2 to accumulate in the recycle streams, with H_2 recovery through a PSA) and a low hydrogen efficiency, because of the large production of water through the reverse WGS reaction. The small CO_2 stream withdrawn from the synthesis loop leads to some emissions and effectively requires a slight oversizing of the DAC to compensate for these losses.

Table 6
Energy and environmental results for the different natural gas based MeOH plants.

Item/Plant	Units	SMR-ATR	ATR-HTER	GSR	Renewable (DAC)
Natural gas	MW_{th}	3236.7	3171.1	2922.4	0.0
Electrolyser duty	MW_{el}	0.0	0.0	0.0	3709.6
MeOH output	kg/s	115.7	115.8	116.0	115.9
MeOH output	MW_{th}	2275.6	2277.2	2280.9	2279.3
Syngas compression	MW_{el}	88.5	64.8	97.4	86.5
CO_2 compression	MW_{el}	0.0	0.0	0.0	68.6
Heat rejection	MW_{el}	3.7	3.1	3.2	0.0
Pumps	MW_{el}	2.9	1.4	0.9	0.4
Blower	MW_{el}	6.4	1.9	0.0	0.0
ASU	MW_{el}	64.8	68.8	0.0	0.0
CPU	MW_{el}	0.0	0.0	0.4	0.0
DAC	MW_{el}	0.0	0.0	0.0	124.3
Total Auxiliaries	MW_{el}	166.3	140.0	101.8	279.8
Steam turbine	MW_{el}	185.5	138.1	4.2	36.3
Gas turbine	MW_{el}	0.0	0.0	22.1	0.0
Net Power	MW_{el}	19.2	−2.0	−75.6	−243.5
$\eta_{El.}$	%	0.6	−0.1	−2.6	–
η_{MeOH}	%	70.3	71.8	78.0	59.5
$\eta_{MeOH,eq}$	%	71.0	71.7	74.9	57.7
ε_C	%	86.7	88.6	94.5	98.6
ε_H	%	90.7	92.6	100.7	67.9
SC	GJ/ton	28.0	27.4	25.2	33.1
SC_{eq}	GJ/ton	27.7	27.4	26.2	34.1
E_{CO_2}	$kgCO_2$/ton	235.3	198.4	76.3	19.1

3.2. Economic results

Economic results are presented in two sections. First the results for conventional technologies and GSR using natural gas feedstock are shown, with dedicated sensitivity analysis results to key process economic assumptions. Secondly, the renewable MeOH plant using renewable power, electrolysis & alternatively DAC or CO_2 from fossil fuel origin is presented for different locations (Germany, Spain, Saudi Arabia & Argentina) and compared to the natural gas routes.

3.2.1. Natural gas MeOH plants

Fig. 4 shows the specific total overnight costs for each of the MeOH plants in k€/tpd. The ATR-HTER configuration reveals 14.2 k€/tpd (-8.9%) lower specific capital costs than the SMR-ATR plant. On the other hand, the GSR concept achieves 21.0 k€/tpd (-13.3%) lower costs than the SMR-ATR benchmark. Relative to the ATR-HTER reference plant, the GSR presents a cost reduction of 4.7%, mainly because avoidance of the ASU offsets the higher costs of the GSR cluster relative to the ATR and HTER. The ATR-HTER plant presents the lowest costs associated to the synthesis loop and purification units, due to the syngas quality produced in this plant that allows a lower pressure operation and decreased reactant recirculation rates. Finally, despite the fact that GSR avoids steam cycle elements, the complex heat recovery network required and gas turbine result in similar power cycle costs as the reference plants. SEA tool files are available for download providing detailed capital and operating cost estimations for each of the cases [60].

Regarding the operating costs for the different configurations, reflected in Fig. 5, the large contribution of natural gas is apparent, amounting to 81.1–82.5% of the total costs. However, the GSR plant achieves a 9.0% and 6.4% lower consumption relative to the SMR-ATR and ATR-HTER configurations, respectively, although this is largely offset by the cost of additional electricity imports. The high carbon conversion efficiency of GSR is responsible for most of its operating cost savings via low CO_2 taxes (3.8% of total costs) relative to the reference plants (9.2–10.6%). GSR also encounters higher variable operational cost due to the large quantities of oxygen carrier replacement.

The LCOM for the different MeOH plants with natural gas feedstock is presented in Fig. 6. The ATR-HTER reference plant is more competitive than the SMR-ATR configuration, achieving a cost reduction of 11.4 €/ton (-4.2%). On the other hand, relative to the ATR-HTER benchmark, the GSR configuration achieves a 16.3 €/ton cost reduction (-6.4%).

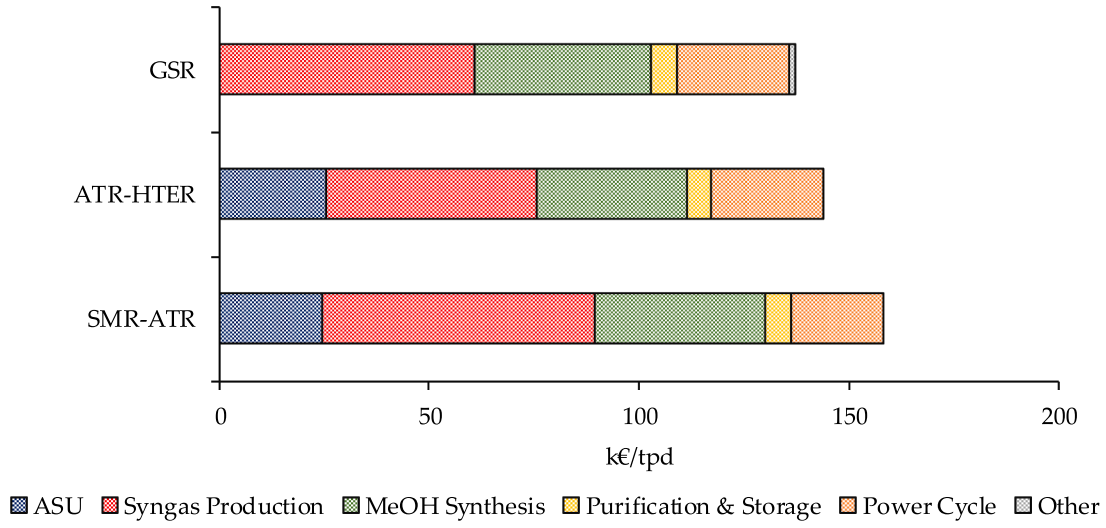

Fig. 4. Specific TOC for the different natural gas based MeOH plants.

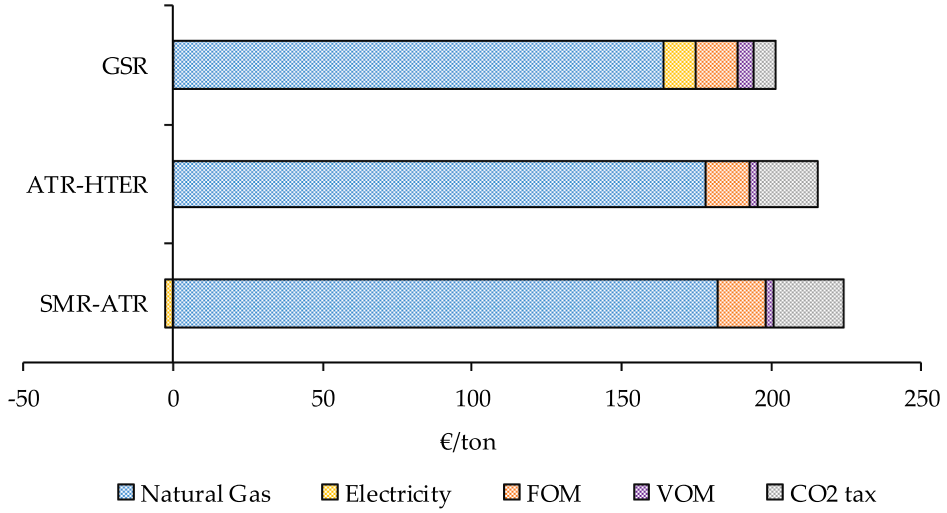

Fig. 5. Specific operating costs for the different natural gas based MeOH plants.

These reductions are achieved through a combination of the factors previously discussed: a better fuel utilization, reduced taxes from CO_2 emissions and lower capital costs (which also result in comparatively lower FOM costs), despite the increase of VOM costs and electricity imports. Overall, it is noteworthy to highlight the large weight of natural gas on the levelized cost for all the cases.

Finally, sensitivity analyses of the LCOM to different economic assumptions are presented in Fig. 7. As expected, the cost is most sensitive to the natural gas price used in the economic evaluation, presenting a somewhat smaller steepness for the GSR due to the slightly higher thermal efficiencies achieved. The CO_2 tax presents a larger effect for both reference plants compared to the GSR configuration, with significantly lower specific emissions. At no CO_2 emissions costs, the GSR configuration is still slightly more competitive than the benchmarks.

Both electricity price and oxygen carrier cost have influence primarily on the GSR configuration, although the effect is small. Finally, the discount rate and capacity factor sensitivities show similar trends for the three cases. The results of the sensitivity reveal the importance of maximizing natural gas conversion efficiency to the final product. This can be a challenging endeavour because some heat will inevitably be lost because of the exothermicity of the synthesis reaction and due to the purge requirements from the loop, either to satisfy the thermal demand of reforming units or to generate sufficient electricity in the steam cycle. For the ATR-HTER reference plant, carbon efficiency could be increased if a combined cycle with a gas turbine were used to generate that power [27], due to higher efficiency electricity generation for a self-sufficient plant, although supply of hot water and low-pressure steam to the MeOH reactor and purification respectively might be compromised.

3.2.2. *Renewable MeOH plants*

The renewable MeOH plants were modelled using GAMS to optimize the investment of capacity and hourly dispatch of technologies for a constant MeOH output of 2300 MW, considering different world regions for renewable energy (wind and solar) availability. Detailed description of the model and assumptions are available in the Supplementary Material file attached to this study, while a file for the results of the cases as well as the model is available online [60].

Fig. 8 shows the optimal capital deployment of technologies built in the four regions. When comparing electricity generation, it can be seen that ARG depends heavily on its outstanding wind resource, both GER and ESP rely on a combination of wind and solar, while SA supplies 100% of the power by solar PV. Since GER and ARG locations present an electricity production mix with an overall higher capacity factor, lower electrolyser capacities are required, especially in ARG where the wind

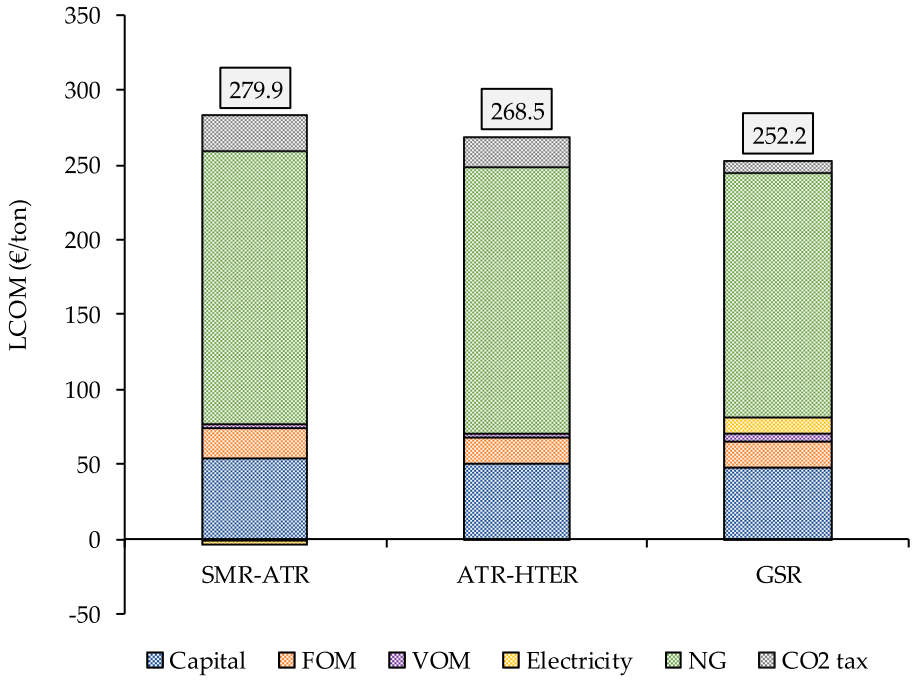

Fig. 6. LCOM for the different natural gas based MeOH plants.

capacity factor exceeds 50%. However, both wind-dominated regions require larger DAC capacity and greater storage volumes of H_2, CO_2 and MeOH, due to the longer variability timescales (random variations on weekly timescales and more regular seasonal variations) of this resource. SA and ESP present substantial battery storage deployment to profit from their low-cost solar resources, while the H_2, CO_2, and MeOH storage comparatively decrease for the last two regions.

The optimal renewable MeOH costs are compared with the natural gas-based plants in Fig. 9. In the European locations, renewable MeOH is cheaper in ESP relative to GER by 229.1 €/ton (-29.2%), in virtue of its solar resource. ESP and ARG present similar costs, being 12.0 €/ton (-2.1%) cheaper in the former. Thus, despite the outstanding wind resource of ARG, the large capital cost reduction assumed for solar PV ensures that the moderately good solar resource in ESP achieves a lower cost of electricity inputs. Another interesting difference between ARG and ESP is the much lower electrolyser cost in the former (due to the high wind capacity factor), partially cancelled out by larger storage costs (due to the longer variability timescales of wind). Owing to its outstanding solar resource, SA achieves the lowest LCOM for the renewable MeOH cases.

For reference, the two renewable MeOH configurations with different CO_2 sources (DAC or CO_2 pipeline) are compared in ARG. As shown in Fig. 9, the DAC plants are credited with a large CO_2 revenue (100 €/ton of CO_2 or 137.5 €/ton of MeOH) for removing CO_2 from the atmosphere, whereas the credit received by the pipeline (CO_2 P/L) option is much smaller (10 €/ton of CO_2 for avoiding the need for CO_2 storage). However, the cost of the DAC system outweighs the large CO_2 credit it generates. Furthermore, the DAC configuration imposes considerably higher renewable electricity costs due to its extra electricity demand and the need to operate the system at a high capacity factor that forces some curtailment of wind energy peaks and deployment of less cost-effective solar. Matching CO_2 supply from DAC with H_2 supply from electrolysis also requires more storage, including CO_2 tanks and CO_2 compressors. The combination of these factors makes the DAC case 62.8 €/ton (+11.1%) more expensive than the pipeline case, illustrating that a CO_2 credit exceeding 100 €/ton will be required to justify DAC under the base case assumptions.

Fig. 9 shows that MeOH from natural gas origin is far cheaper than that of renewable origin, despite the CO_2 price/credit of 100 €/ton. In Europe, natural gas pathways are 287.4 €/ton (-51.7%) and 303.6 €/ton (-54.6%) cheaper than renewable MeOH from ESP with the ATR-HTER and GSR plants, respectively. This difference is even larger in SA where the improved solar resource is outweighed by low fuel prices in this natural gas exporting region Specifically, the ATR-HTER and GSR plants achieve drastic cost reductions of 326.4 €/ton (-69.2%) and 336.3 €/ton (-71.3%), respectively, relative to the renewable MeOH case. The renewable cases for ARG location are not directly benchmarked against natural gas feedstock plants under the consideration that for this world region, NG prices will be similar to Europe. Since its LCOM is slightly higher than that of ESP, the comparison to NG cases will be less favourable.

It must also be noted that these estimations present an optimistic scenario for the renewable plants, since only one year of energy source variability is considered for the optimization, and it is assumed that the plant can be operated with perfect foresight across regarding wind and solar power production. Furthermore, all technologies within the renewable plants are assumed to operate with full availability, relative to the 85% capacity factor taken for the natural gas-based plants. Given the cost projection uncertainties for the different technologies considered to the year 2050, and the possibility of alternatively utilizing CO_2 available from pipeline, sensitivity cases outlined in Table 5 are presented in Fig. 10 for all locations, re-running the optimization for each case with suitable model modifications (e.g., pipeline CCU cases do not require CO_2 storage, compression etc.).

GSR natural gas based MeOH plants remain far more competitive than the renewable MeOH plants with optimistic technology assumptions for all locations. For ARG location, the GSR plant estimation for Europe is represented in Fig. 10 for perspective. Also, at a CO_2 tax of 100 €/ton, plants with CCU are economically more attractive than investment in DAC for all locations, although this difference becomes smaller for SA and ESP, due to less CO_2 storage and compression requirements in those regions. In general, variations between high and low levels for DAC has the greatest impact on LCOM, with a greater comparative cost increase at the high level imposed by larger thermal and electricity auxiliary demands on the DAC, which in turn imply higher investments in power and heat generation and storage. Next, changes in the capital cost of the primary energy input have a substantial influence, particularly for those regions largely depending on their wind resource.

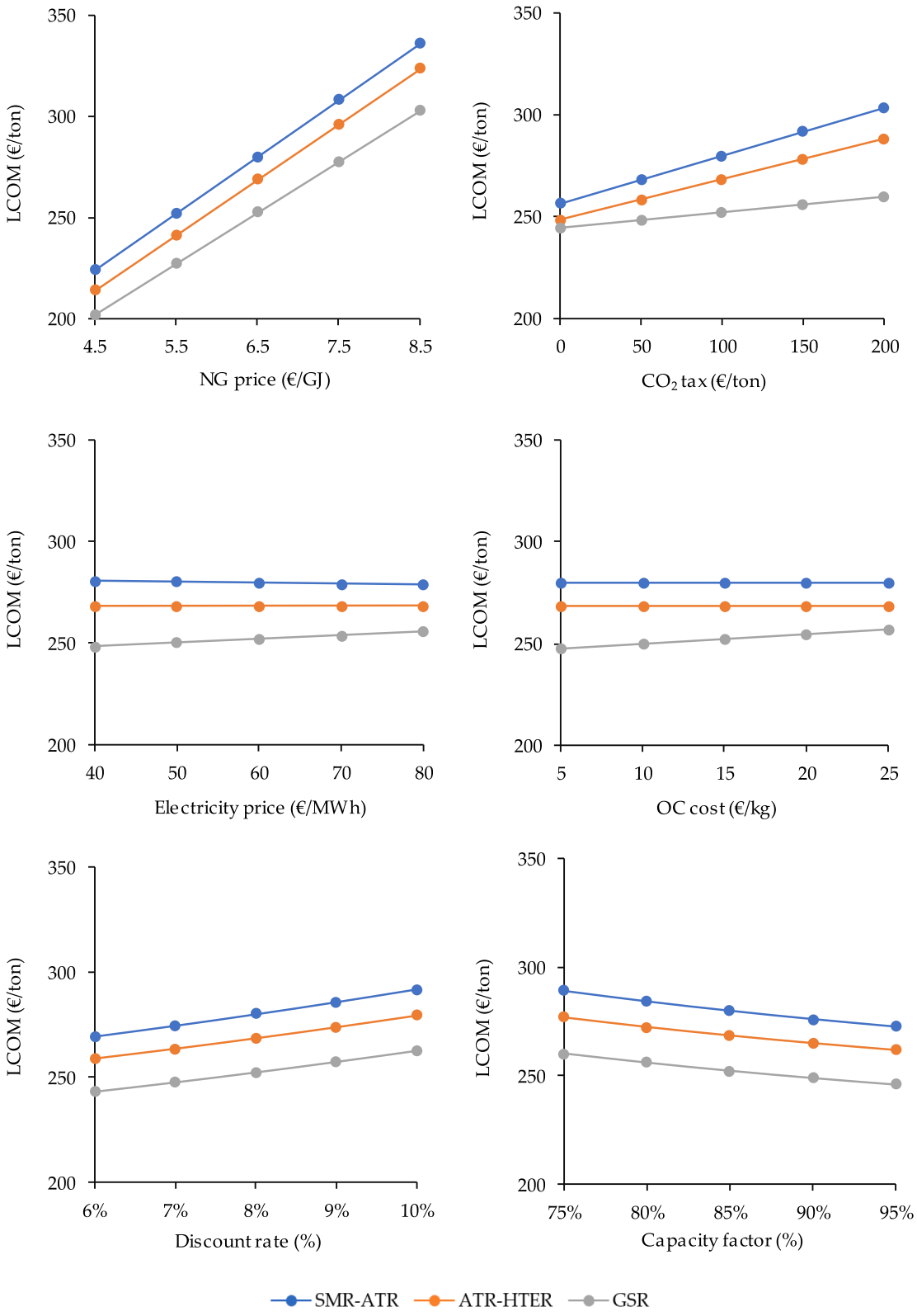

Fig. 7. LCOM sensitivity analysis to different economic assumptions.

Electrolyser cost is less influential, although still considerable in solar-dominated regions due to the large oversizing required to utilize daily solar production peaks.

Finally, it is clarifying to identify the break-even CO_2 prices which make the renewable MeOH plants with DAC comparable in terms of levelized cost to the a) CO_2 from pipeline case and b) the NG plants. Notably, the CO_2 price also impacts both latter configurations, as the carbon conversion in the synthesis loop of each plant is below 100%, causing some emissions. These CO_2 prices are represented relative to each technology and location in Fig. 11:

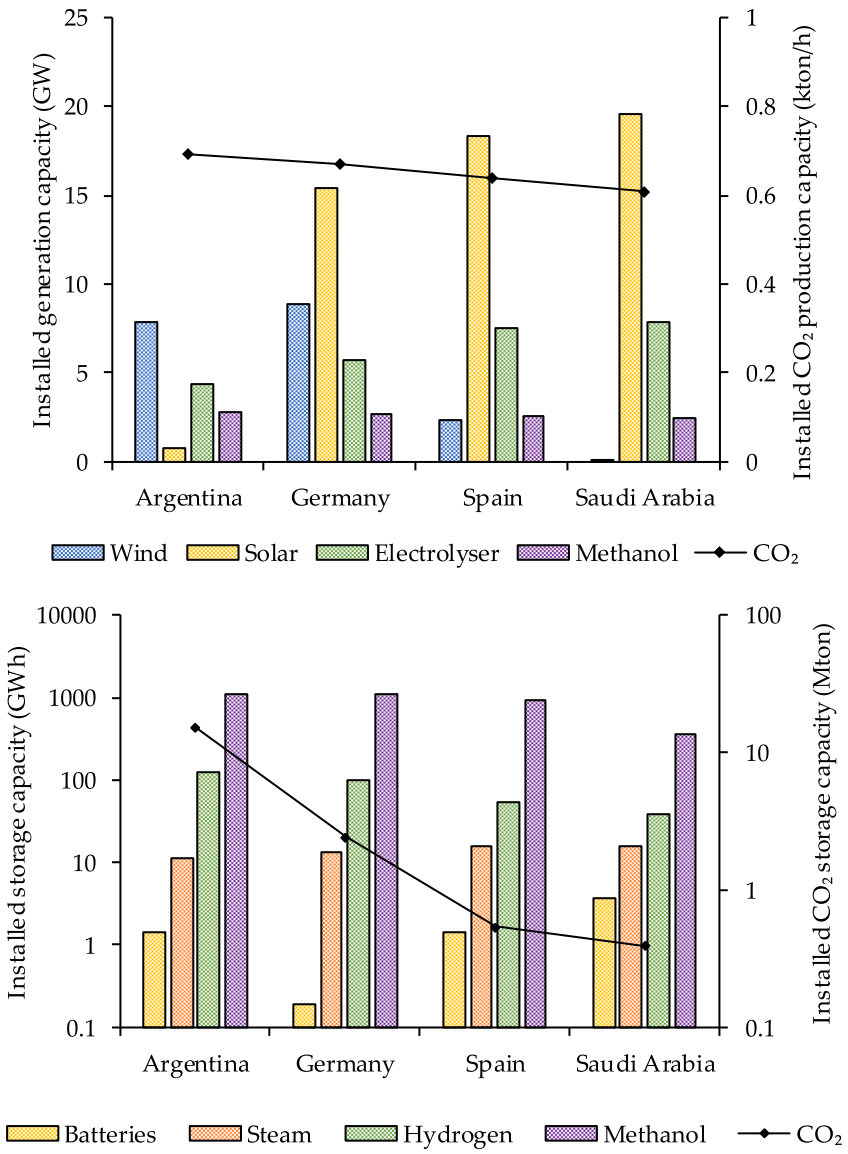

Fig. 8. Optimal generation (above) and storage (below) capital deployment for the renewable MeOH with DAC for the different regions. The storage figure presents a logarithmic axis due to the large differences in deployment.

As expected, huge CO_2 taxes above 318.0 €/ton (ESP) are required for renewable MeOH with DAC to outcompete the advanced NG-based GSR configuration, while DAC can economically replace pipeline CO_2 in the renewable cases if CO_2 prices reach ranges between 121.3 and 146.7 €/ton, depending on the location. Given the larger emissions and relative higher cost of the ATR-HTER plant, the break-even prices of the DAC with respect to this technology are somewhat smaller, with the lowest of 290.3 €/ton reached for ESP location. Finally, the robustness of the conclusion that NG-based MeOH is much cheaper than renewable MeOH is verified by completing a simulation in ESP where optimistic cost assumptions are applied to all green technologies. In this case, a CO_2 tax of 162.8 €/ton is required for renewable MeOH to outcompete MeOH from the GSR process.

3.2.3. *Comparison to NH_3 as a future energy carrier*

Given the growing relevance of alternative energy carriers in a decarbonized economy, the results of this study for MeOH are compared to a previous work that applied an identical methodology for the assessment of NH_3 [39]. In this previous work, an evaluation of the GSR-NH_3 production process was carried out for a 3000 tpd capacity, in which H_2 is obtained from a PSA after a WGS unit. Additionally, N_2 from the oxidation stage GSR outlet is added to the synthesis loop after a purification step. The PSA off-gas is recirculated to the GSR reduction step, thereby capturing a CO_2 stream for transport and storage after water knock out and purification. On the other hand, the MeOH plant design does not require CO_2 transport and storage because most of the CO_2 from the GSR reduction step is fed back to the reforming step to maximize the carbon conversion efficiency, while the N_2 stream from the GSR is vented after expansion and heat recovery. For the NH_3 process using renewable power as primary energy feedstock, N_2 reactant is produced from a dedicated cryogenic unit, compared to DAC in the MeOH counterpart for CO_2, while the same electrolyser, wind, solar, battery, and H_2 storage technology is assumed in both plants.

Fig. 12 shows the techno-economic results for SA location on an energy basis. This natural gas exporting region with high solar availability returned the lowest costs both for renewable and natural gas routes, making it an ideal location for the export of cleaner energy carriers over coming decades. No CO_2 tax benefit was considered in this comparison for renewable MeOH (with DAC), considering that this energy carrier will release the CO_2 captured via DAC at the end-use, making it directly comparable to green NH_3 for energy applications.

The results show that, for the renewable route, ammonia is 15.3

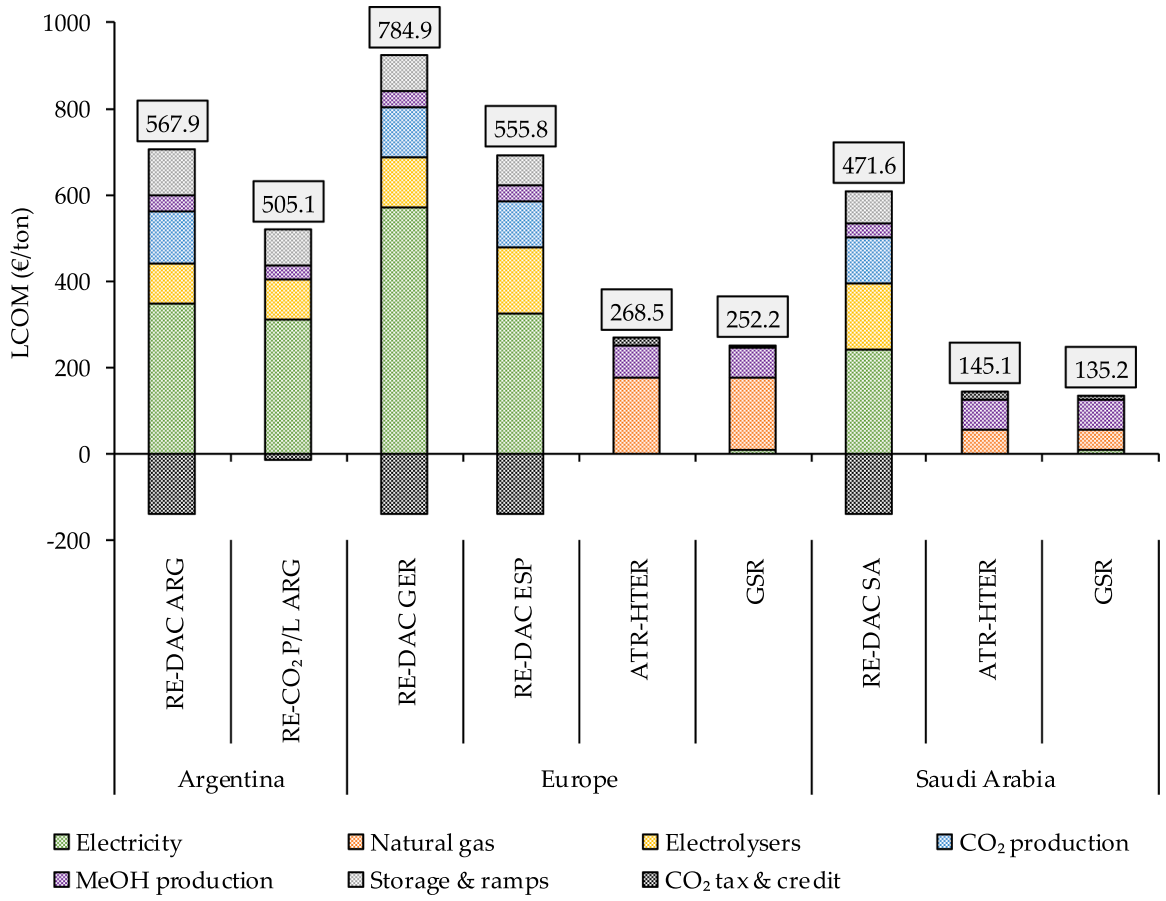

Fig. 9. LCOM comparison for the different MeOH production pathways. Total costs are indicated above the bars accounting for a 100 €/ton CO_2 taxes for the renewable plants with DAC and natural gas plants, and 10 €/ton CO_2 credit for the CCU case.

€/MWh (-13.7%) cheaper than MeOH. Even though the MeOH synthesis loop is considerably simpler than the NH_3 loop, the additional requirement for DAC puts green MeOH at a significant cost disadvantage to green NH_3. On the other hand, when using a natural gas feedstock, MeOH is more attractive as an energy carrier by 12.5 €/MWh (–33.6%), as larger production and simpler synthesis loop achieve more attractive economies of scale. Nevertheless, assuming the MeOH energy carrier produced from natural gas is used in energy applications without CO_2 abatement, a CO_2 tax of 274.3 and 49.8 €/ton would make green and blue ammonia an economically competitive alternative, respectively.

4. Summary & conclusions

Several MeOH production pathways were analysed in this work, carrying out a consistent techno-economic assessment for production capacities of 10,000 tpd. Three natural gas-based plant models were developed. Two benchmark MeOH technologies, one employing steam methane reforming followed by autothermal reforming (SMR-ATR) for syngas production integrating the synthesis loop purge with the reformer, and another with an autothermal reformer operating in parallel with a heat transfer exchanger reformer (ATR-HTER) syngas production section with a steam cycle boiler for combustion of the synthesis purge. A third configuration with natural gas feedstock employing gas switching reforming (GSR) was also assessed. Finally, plants based on H_2 from water electrolysis with renewable electricity and CO_2 from direct air capture (DAC) or alternatively CO_2 utilization from other fossil sources, as means to supply reactants to the synthesis loop, were also the object of this study. The main results of this study are summarized below:

- In terms of technical performance, the SMR-ATR configuration achieved an equivalent specific consumption of 27.7 GJ/ton with electricity exports representing 0.6% of the total heat input. The ATR-HTER plant with net zero electricity demand presented 27.4 GJ/ton specific consumption, while the GSR requires lower equivalent specific consumption of 26.2 GJ/ton of which 4% represents electricity imports. The GSR configuration also achieved low CO_2 emissions of 76.3 kg/ton, a 61.5% reduction relative to the ATR-HTER benchmark. Due to conversion losses in the electrolyzer, synthesis loop, and the power consumption of the DAC facility, the specific electricity consumption of the renewable MeOH plant was higher at 34.1 GJ/ton, albeit with no CO_2 emissions.
- The subsequent economic assessment revealed that the SMR-ATR plant achieved a levelized cost of MeOH (LCOM) of 279.9 €/ton, while the ATR-HTER plant brought a 11.4 €/ton (-4.2%) reduction and GSR lowered costs by an additional 16.3 €/ton (-6.4%) relative to ATR-HTER. Natural gas price and CO_2 tax were the most influential economic assumptions affecting the cost of each plant.
- Using cost assumptions applicable to 2050 for green energy production and storage technology and a DAC CO_2 capture credit of 100 €/ton, renewable MeOH production remained substantially more costly than natural gas-based alternatives. In Spain and Saudi Arabia, the GSR process is 54.6% and 71.9% cheaper than the renewable route, respectively. CO_2 utilization from available fossil fuel sources proved more competitive than DAC route at CO_2 taxes of 100 €/ton. Break even CO_2 taxes for renewable DAC relative to CO_2 from pipeline were found to be in the range of 121.3–146.7 €/ton, while prices around 300 €/ton of CO_2 are required for DAC to make commercial sense with respect to conventional natural gas production routes. Assuming the most optimistic cost prospects for all

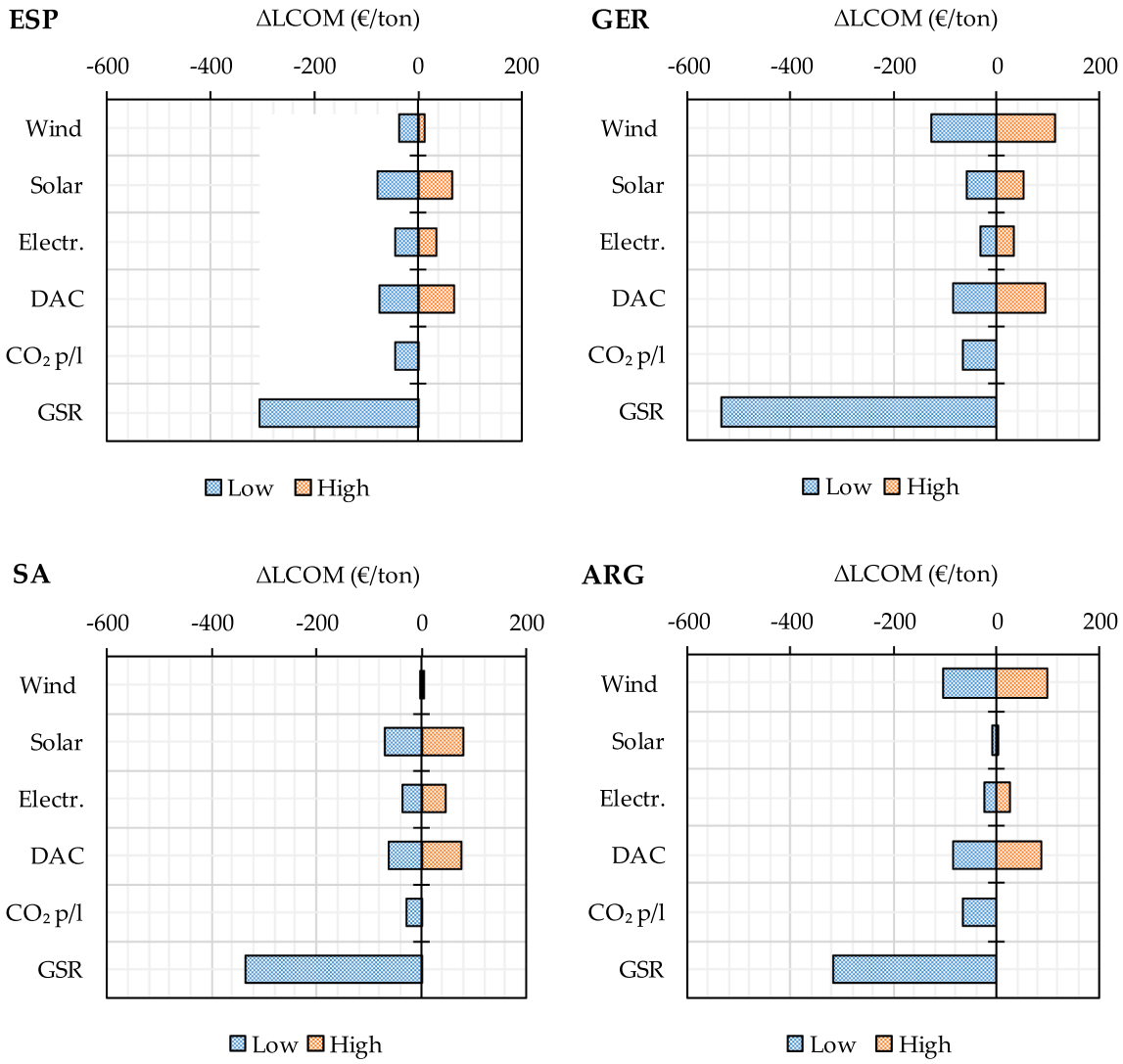

Fig. 10. Sensitivity study to LCOM of technology costs and production alternatives (CO_2 from pipeline, GSR) for renewable MeOH production with DAC in different locations.

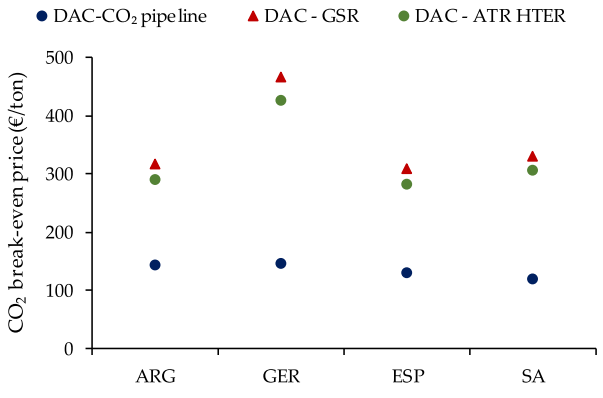

Fig. 11. Break even CO_2 prices for renewable MeOH plants with DAC relative to CO_2 from pipeline and GSR configuration.

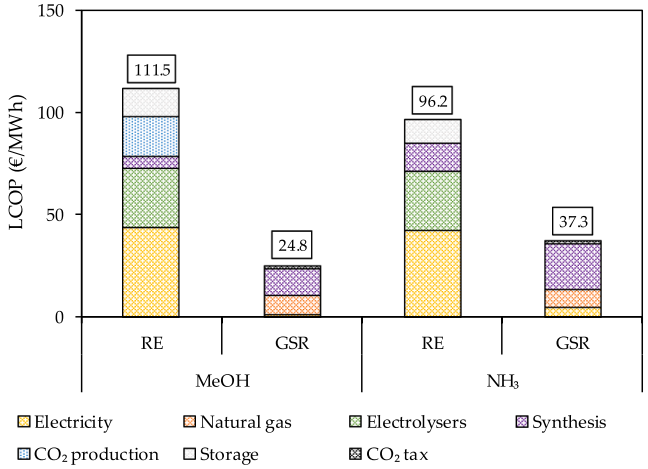

Fig. 12. LCOP in €/MWh for chemical energy carriers from renewables and natural gas in Saudi Arabia.

technologies in the renewable MeOH plant for Spain, the break-even CO_2 tax fell to 163.6 €/ton, relative to a GSR plant.

Finally, MeOH and NH_3 as future energy carriers were compared

using the same methodology, revealing that MeOH presents better economies of scale if produced from natural gas, while the avoidance of DAC makes ammonia the cheaper option for renewable routes. CO_2 taxes for emissions derived from MeOH from natural gas origin of 274.1 €/ton and 49.8 €/ton make green and blue ammonia more compelling as an energy carrier respectively, assuming an identical energy-related end use for such fuels.

In conclusion, it is expected that natural gas-based MeOH production through the state-of-the-art ATR-HTER route will remain more competitive than renewable synthesis based on electrolysis and direct air capture or captured CO_2 utilization in the long term, despite the environmental attractiveness of a CO_2 closed loop fuel production process that DAC route enables. Thus, strong policy support will be required to enable the large-scale production of green MeOH, even in the long term. Advanced process routes like GSR can achieve further cost reductions relative to the ATR-HTER benchmark, but step-changes in natural gas-based MeOH production costs appear unlikely. GSR is better suited to applications like blue H_2 and NH_3 production where its inherent CO_2 capture ability is better utilized.

CRediT authorship contribution statement

Carlos Arnaiz del Pozo: Conceptualization, Methodology, Formal analysis, Investigation, Writing – original draft, Funding acquisition. **Schalk Cloete:** Conceptualization, Methodology, Formal analysis, Investigation, Writing – original draft, Writing – review & editing, Funding acquisition. **Ángel Jiménez Álvaro:** Writing – review & editing, Funding acquisition.

Declaration of Competing Interest

The authors declare that they have no known competing financial interests or personal relationships that could have appeared to influence the work reported in this paper.

Acknowledgements

The authors would like to acknowledge Honeywell for the free academic license of Unisim Design R481. The authors would also like to acknowledge AmsterCHEM for the free academic license of the CAPE-OPEN Scilab-Unisim unit operation. This work received funding from the European Union NextGenerationEU, Ministerio de Universidades grant RD 289/2021.

Appendix A. Supplementary data

Supplementary data to this article can be found online at https://doi.org/10.1016/j.enconman.2022.115785.

References

[1] Basile A, Dalena F. Methanol: Science and Engineering; 2017.
[2] Anonymous European Geosciences Union's Reaction to IPCC Report on Global Warming of 1.5 Degrees Celsius. Targeted News Service; 2018.
[3] Revankar ST. Chapter Six – Chemical Energy Storage; 2019, pp. 177–227.
[4] Mazloomi K, Gomes C. Hydrogen as an energy carrier: prospects and challenges. Renew Sustain Energy Rev 2012;16(5):3024–33.
[5] Schüth F. Challenges in hydrogen storage. Eur Phys J Special Topics; 2009, 176 (1), 155–66.
[6] Abdalla AM, Hossain S, Nisfindy OB, Azad AT, Dawood M, Azad AK. Hydrogen production, storage, transportation and key challenges with applications: a review. Energy Convers Manage 2018;165:602–27.
[7] Olah GA. Beyond oil and gas: the methanol economy. Angew Chem Int Ed. 2005;44 (18):2636–9.
[8] Verhelst S, Turner JW, Sileghem L, Vancoillie J. Methanol as a fuel for internal combustion engines. Prog Energy Combust Sci 2019;70:43–88.
[9] Tola V, Lonis F. Low CO2 emissions chemically recuperated gas turbines fed by renewable methanol. Appl Energy 2021;298.
[10] Alias MS, Kamarudin SK, Zainoodin AM, Masdar MS. Active direct methanol fuel cell: an overview. Int J Hydrogen Energy 2020;45(38):19620–41.
[11] Rivera-Tinoco R, Farran M, Bouallou C, Auprêtre F, Valentin S, Millet P, Ngameni JR. Investigation of power-to-methanol processes coupling electrolytic hydrogen production and catalytic CO2 reduction. Int J Hydrogen Energy 2016;41 (8):4546–59.
[12] Ravikumar D, Keoleian G, Miller S. The environmental opportunity cost of using renewable energy for carbon capture and utilization for methanol production. Appl Energy 2020;279.
[13] Kotowicz J, Węcel D, Brzęczek M. Analysis of the work of a "renewable" methanol production installation based ON H2 from electrolysis and CO2 from power plants. Energy 2021;221.
[14] Battaglia P, Buffo G, Ferrero D, Santarelli M, Lanzini A. Methanol synthesis through CO2 capture and hydrogenation: thermal integration, energy performance and techno-economic assessment. J CO2 Util 2021;44.
[15] Bos MJ, Kersten SRA, Brilman DWF. Wind power to methanol: renewable methanol production using electricity, electrolysis of water and CO2 air capture. Appl Energy 2020;264.
[16] Schorn F, Breuer JL, Samsun RC, Schnorbus T, Heuser B, Peters R, Stolten D. Methanol as a renewable energy carrier: An assessment of production and transportation costs for selected global locations. Advances Appl Energy 2021;3.
[17] Bozzano G, Manenti F. Efficient methanol synthesis: perspectives, technologies and optimization strategies. Prog Energy Combust Sci 2016;56:71–105.
[18] Ghosh S, Seethamraju S. Process intensification with a polar solvent in liquid phase methanol synthesis. Proc Integr Optimiz Sustainability 2021;5(4):827–42.
[19] Lee S. Methanol synthesis technology; 1989.
[20] Gallucci F. Inorganic Membrane reactors for methanol synthesis. 2018, 493–518.
[21] Salehi M, Askarishahi M, Gallucci F, Godini HR. Selective CO2-hydrogenation using a membrane reactor. Chem Eng Process-Process Intensif. 2021;160.
[22] Rydén M, Lyngfelt A, Mattisson T. Synthesis gas generation by chemical-looping reforming in a continuously operating laboratory reactor. Fuel 2006;85(12): 1631–41.
[23] Zaabout A, Cloete S, Johansen ST, Van SA, Gallucci F, Amini S. Experimental demonstration of a novel gas switching combustion reactor for power production with integrated CO 2 capture. Ind Eng Chem Res 2013;52(39):14241–50.
[24] Nazir SM, Cloete JH, Cloete S, Amini S. Pathways to low-cost clean hydrogen production with gas switching reforming. Int J Hydrogen Energy 2020.
[25] Wassie SA, Gallucci F, Zaabout A, Cloete S, Amini S, van Sint Annaland M. Hydrogen production with integrated CO2 capture in a novel gas switching reforming reactor: proof-of-concept. Int J Hydrogen Energy 2017;42(21): 14367–79.
[26] Abad A, Adánez J, García-Labiano F, de Diego L, Gayán P, Celaya J. Mapping of the range of operational conditions for Cu-, Fe-, and Ni-based oxygen carriers in chemical-looping combustion. Chem Eng Sci 2007;62(1–2):533–49.
[27] Osman M, Zaabout A, Cloete S, Amini S. "Pressurized chemical looping methane reforming to syngas for efficient methanol production: experimental and process simulation study. Adv Appl Energy 2021;4.
[28] Spallina V, Motamedi G, Gallucci F, van Sint Annaland M. Techno-economic assessment of an integrated high pressure chemical-looping process with packed-bed reactors in large scale hydrogen and methanol production. Int J Greenhouse Gas Control 2019;88:71–84.
[29] Labbaf B, Tabatabaei M, Mostafavi E, Tijani M, Mahinpey N. Methanol production via integrated methane reforming and chemical looping combustion: process simulation and techno-economic assessment. Process Saf Environ Prot 2021;148: 1346–56.
[30] Osat M, Shojaati F. Techno-economic-environmental evaluation of a combined tri and dry reforming of methane for methanol synthesis with a high efficiency CO2 utilization. Int J Hydrogen Energy 2022;47(14):9058–70.
[31] Blumberg T, Lee YD, Morosuk T, Tsatsaronis G. Exergoenvironmental analysis of methanol production by steam reforming and autothermal reforming of natural gas. Energy 2019;181:1273–84.
[32] Collodi G, Azzaro G, Ferrari N, Santos S. Demonstrating large scale industrial CCS through CCU–a case study for methanol production. Energy Procedia 2017;114: 122–38.
[33] Wesenberg MH. Gas heated steam reformer modelling; 2006.
[34] Aasberg-Petersen K, Nielsen CS, Dybkjær I, Perregaard J. Large scale methanol production from natural gas. Haldor Topsoe 2008;22.
[35] Woods M, Kuehn N, Shah V, Goellner JF. Baseline analysis of crude methanol production from coal and natural gas. NETL 2014.
[36] Blumberg T, Morosuk T, Tsatsaronis G. A comparative exergoeconomic evaluation of the synthesis routes for methanol production from natural gas. Appl Sci 2017;7 (12):1213.
[37] Honeywell, Unisim Thermo Reference Guide R480 Release; 2020.
[38] Moriya N, Kawai T, Yagi H, Shimizu R, Morita Y. Method of heat transfer in reformer; 1999.
[39] Arnaiz del Pozo C, Cloete S. Techno-economic assessment of blue and green ammonia as energy carriers in a low-carbon future. Energy Convers Manage 2022; 255.
[40] Campanari S, Mastropasqua L, Gazzani M, Chiesa P, Romano MC. Predicting the ultimate potential of natural gas SOFC power cycles with CO2 capture – Part A: methodology and reference cases. J Power Sources 2016;324:598–614.
[41] FCH. State of the art and future targets for fuel cell and hydrogen applications, https://www.fch.europa.eu/soa-and-targets [accessed on 02.11.2021].
[42] Grigoriev SA, Porembsky VI, Fateev VN. Pure hydrogen production by PEM electrolysis for hydrogen energy. Int J Hydrogen Energy 2006;31(2):171–5.
[43] Fasihi M, Efimova O, Breyer C. Techno-economic assessment of CO2 direct air capture plants. J Clean Prod 2019;224:957–80.
[44] Anonymous. https://climeworks.com/purpose. Accessed: March 2020.

[45] Kauko H, Sevault A, Beck A, Drexler-Schmid G, Schöny M. Cost-efficient thermal energy storage for increased utilization of renewable energy in industrial steam production – CETES. Available from: https://bit.ly/3COrgtj; 2020.
[46] De María R, Díaz I, Rodríguez M, Sáiz A. Industrial methanol from syngas: kinetic study and process simulation. Int J Chem Reactor Eng 2013;11(1):469–77.
[47] Slotboom Y, Bos MJ, Pieper J, Vrieswijk V, Likozar B, Kersten SRA, Brilman DWF. Critical assessment of steady-state kinetic models for the synthesis of methanol over an industrial Cu/ZnO/Al2O3 catalyst. Chem Eng J 2020;389.
[48] Bussche KMV, Froment GF. A steady-state kinetic model for methanol synthesis and the water gas shift reaction on a commercial Cu/ZnO/Al2O3 catalyst. J Catal 1996;161(1):1–10.
[49] Seidel C, Jörke A, Vollbrecht B, Seidel-Morgenstern A, Kienle A. Kinetic modeling of methanol synthesis from renewable resources. Chem Eng Sci 2018;175:130–8.
[50] Prašnikar A, Pavlišič A, Ruiz-Zepeda F, Kovač J, Likozar B. Mechanisms of copper-based catalyst deactivation during CO2 reduction to methanol. Ind Eng Chem Res 2019;58(29):13021–9.
[51] Halager NS, Bayer C, Kirkpatrick R, Gernaey KV, Huusom JK, Udugama IA. Modelling and control of an integrated high purity methanol distillation configuration. Chem Eng Process – Process Intensif 2021;169.
[52] Khan MN, Cloete S, Amini S. Efficiency improvement of chemical looping combustion combined cycle power plants. Energy Technol 2019;7(11):1900567.
[53] Carlos Arnaiz del Pozo, Schalk Cloete, and Ángel Jiménez Álvaro. Standard Economic Assessment (SEA) Tool. Available from: https://bit.ly/3hyF1TT.
[54] Turton R, Bailie RC, Whiting WB, Shaeiwitz JA. Analysis, synthesis and design of chemical processes; 2008.
[55] Carlos Arnaiz del Pozo, Schalk Cloete and Ángel Jiménez Álvaro. SEA Tool User Guide. Available from: https://bit.ly/3jq9Bkf.
[56] Roussanaly S, Berghout N, Fout T, Garcia M, Gardarsdottir S, Nazir SM, Ramirez A, Rubin ES. Towards improved cost evaluation of carbon capture and storage from industry. Int J Greenhouse Gas Control 2021;106.
[57] Anantharaman R, Bolland O, Booth N, Van Dorst E, Sanchez Fernandez E, Franco F, et al., Cesar deliverable D2.4.3. European best practice guidelines for assessment of Co2 capture technologies; 2018.
[58] Pfenninger S, Staffell I. Long-term patterns of European PV output using 30 years of validated hourly reanalysis and satellite data. Energy 2016;114:1251–65.
[59] Fasihi M, Efimova O, Breyer C. Techno-economic assessment of CO2 direct air capture plants. J Clean Prod 2019;224:957–80.
[60] Arnaiz del Pozo C, Cloete S, Jiménez Álvaro Á. Methanol pathways: SEA tool files and System-scale model results. Available from: https://bit.ly/3Nzdpv0; 2022.